






Research Article

Study of the Mechanical and Microscopic Properties of Modified Silty Clay under Freeze-Thaw Cycles

Zhou Wenjun ¹, Wang Qingzhi ^{1,2}, Fang Jianhong ², Wang Kejin ³
and Zhao Xiangqing ⁴

¹Qinghai University, Civil Engineering College, Xining, Qinghai 810016, China

²Qinghai Research and Observation Base, Key Laboratory of Highway Construction & Maintenance Technology in Permafrost Region, Ministry of Transport, Xining, Qinghai 810016, China

³Qinghai Highway Construction Administration, Xining, Qinghai 810016, China

⁴Northwest Research Institute Co. Ltd of C.R.E.C, Lanzhou, Gansu 730000, China

Correspondence should be addressed to Wang Qingzhi; wangqingzhi87@qhu.edu.cn

Received 25 January 2022; Accepted 25 February 2022; Published 14 March 2022

Academic Editor: Tao Chen

Copyright © 2022 Zhou Wenjun et al. This is an open access article distributed under the Creative Commons Attribution License, which permits unrestricted use, distribution, and reproduction in any medium, provided the original work is properly cited.

Silty clay can be found in the alpine region of the Qinghai province, China, where it is subject to annual freeze-thaw cycles. To investigate the static mechanical properties of silty clay modified by basalt fiber and basalt powder under the action of freeze-thaw cycles, triaxial compression tests and scanning electron microscope tests were conducted on the soil. The test results revealed that varying the number of freeze-thaw cycles resulted to different effects on the soil mechanical strength, which tended to increase after 2 cycles, but then tended to decline when subjected to 5–10 cycles. After 20 freeze-thaw cycles, soil strength reached a dynamic equilibrium state. The shear strength of basalt fiber soil and basalt powder soil increased by 7.55% and 5.12%, respectively, compared with that of normal soil under 30 freeze-thaw cycles. Subsequently increasing of the number of freeze-thaw cycles differentially affected the cohesion and internal friction angle of normal soil and admixture soils, and these soils gradually tended to stabilize at a mechanical strength higher than the initial value. Basalt fibers reinforced the soil to a higher degree than basalt powder at a dosage of 0.4% based on dry soil mass. The stress-strain curves of the three soil types can be simulated using the hyperbolic model. The results of the study can provide some theoretical reference for practical engineering in seasonal frozen soil areas.

1. Introduction

Rapid global warming is severely degrading permafrost at a worldwide scale, turning permafrost into seasonally frozen soil gradually. China has the third largest amount of permafrost in the world, in which the percentage of permafrost in the Qinghai-Tibet Plateau region is relatively large. In recent years, due to the needs of national development, many places rarely visited by people before began to be developed, especially that the development of transportation has accelerated the degradation of permafrost. On the one hand, the construction of roads, railroads, and other transportation projects affects the original state of the natural environment;

on the other hand, the change of the road environment will also affect the normal use of engineering buildings.

The seasonal frozen soil and reinforced soil problem has been carried out by many scholars, for example, the strength of the soil after freeze-thaw cycles, the effect of different freeze-thaw cycles on the soil, and the modification method. To study the undrained strength of clay, Fabian and Fourie [1] added geotextiles with different permeability coefficients to silty clay, finding that the geotextile reinforcement material with high permeability had better effect on soil strength. Similar reinforcement experiments on sandy soils revealed that incorporating fibers can increase the strength of soil [2]. Others have found that polypropylene fiber can substantially

bolster soil reinforcement [3–8]. Hejazi et al. [9] reviewed the history, benefits, applications, and possible problems that may arise from using different types of natural or synthetic fibers in soil reinforcement. This meta-analysis supports the overarching idea that the strength and stiffness of admixture soils are improved by fiber. Geotextile layers reinforcing soils were further found to reduce the effects of freeze-thaw cycles on changes of soil cohesion and resilient modulus [10]. Other studies have tested the use of additives including waste materials such as lime and rice husk ashes to improve the geotechnical properties of an expansive clay soil subject to freeze-thaw effect, finding that the effects on soil behavior were positive [11]. Using polymer stabilization to create a new nanocomposite material with clay soil has been found to effectively stabilize slopes and road embankments [12, 13]. Delinière et al. [14] deal with the characterization of five ready-mixed clay plasters from French brickworks using the recent German standard. Basalt, glass, and steel fibers have been added to fine-grained soils to improve thermal conductivity, producing close matches between the values estimated by a statistical-physical model [15].

Innocent Kafodya and Okonta [16] investigated the synergic effects of precompression and fiber inclusions on the mechanical behavior of lime fly ash-stabilized soil, finding that the optimum strength of 3.5 MPa was generated from unprecompressed specimens at a 0.75% fiber content. Others examining the reuse of waste tire textile fibers (WTF) to reinforce soils suggest that WTF improve all strength and ductility parameters of sandy soil [17]. Soil samples reinforced with tire rubber fiber exhibited decreasing liquid limits, dry density, swell potentials, and swelling pressure as tire rubber fiber content and cement increase [18]. The addition of nanocalcium carbonate as a stabilizing nanoparticle and carpet waste fibers as a reinforcement agent to clayey soils reduced their liquid limit and increases its plastic limit [19]. Other studies investigating the effect of silica fume and polypropylene fiber modification on the strength and freeze-thaw behavior of lime-stabilized kaolinite clay have found that these reinforced clays can be an economic and environmentally friendly alternative in soil stabilization projects [20]. Based on results of Tanzadeh et al. [21], the optimal weight percentages for lime powder and lime nanoparticles were approximately 4 and 1, respectively, when they were combined with clay. The swelling pressure, expansion percentage, and time rate of swell decrease, whereas the unconfined compressive strength (UCS) increases with the addition of expanded polystyrene (EPS) to soils [22]. Silica fume (SF) and polypropylene (PP) have been shown to be effective at reinforcing soils and show promise in environmentally friendly road work applications [23]. Almajed et al. [24] investigated the optimal levels of reinforcement fiber length (FL), fiber dosage (FD), and curing time (CT) for geotechnical parameters of stabilized soil and pointed optimal values of these indicators.

The above studies illustrate that most of the tests have focused on the effects of adding a single reinforcing material to the soil; far fewer examine the addition of multiple different materials or compare their effects under identical

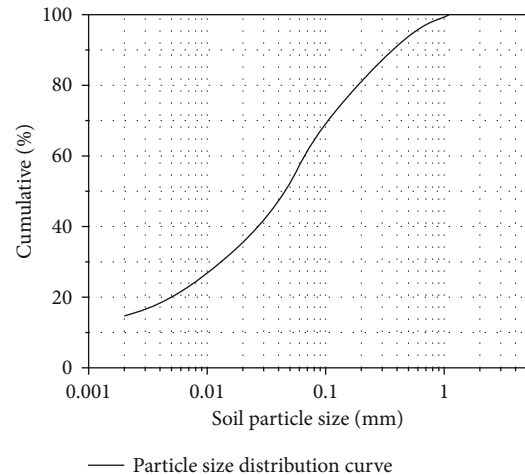


FIGURE 1: Particle gradation curve of the soil used in the test.

test conditions. Modifications under freeze-thaw cycling conditions are also rare. For example, fiber additions focus almost solely on polypropylene fiber and the research on other fiber materials is still lacking. Experimental research on the effects of freeze-thaw cycle conditions on these modified materials is even scarcer. Furthermore, existing studies largely ignore the effects of diurnal temperature differences, differences in quarterly average temperatures, and the number of freeze-thaw cycles on the soil in alpine regions. To address the above issues, this paper will investigate the static mechanical properties and microstructure change characteristics of the soil after incorporating basalt fiber and basalt powder under different numbers of freeze-thaw cycles by triaxial compression test and scanning electron microscope test.

2. Test Materials and Protocol

2.1. Sampling Location. The test sampling site is the Jingyangling section of the Bianmen Expressway. The route, which runs northwest to southeast, starts near the maintenance boundary of Qing-Gan Highway in Biandukou and connects with the Zhangye-Biandukou Expressway planned by Gansu province, which belongs to seasonal frozen regions. Soil was collected from extraction pile number K42+650, in Qinghai Haibei Tibetan Autonomous Prefecture. After a series of physical properties tests, the soil was classified as silty clay (Figure 1; Table 1; Highway Geotechnical Test Procedure JTG 3430-2020).

2.2. Modified Materials. Basalt fiber has the characteristics of green environmental protection, and basalt powder has large reserves, strong hardness, and easy to obtain. In this experiment, basalt fiber and basalt powder were added to the silty clay to modify it. The physical and chemical parameters of these substances are shown in Tables 2 and 3.

The morphology of the two modified materials is shown in Figure 2.

2.3. Soil Sample Preparation. The test soil sample was collected in an 80 mm × 39.1 mm (height × diameter) cylinder.

TABLE 1: Physical properties of soil samples.

Natural moisture content w (%)	Plastic limit w_p (%)	Liquid limit w_L (%)	Plasticity index I_p	Maximum dry density ρ_{dmax} (g/cm ³)	Optimal moisture content w_{op} (%)
11.72	16.1	22.3	6.2	2.05	10.20

TABLE 2: Physical and chemical parameters of basalt fibers.

Fiber type	Density (g·m ⁻³)	Length (mm)	Monofilament diameter (μ m)	Tensile strength (MPa)	Operating temperature ($^{\circ}$ C)	Acid and alkali resistance	Dispersion
Filamentous	2.64	9	15	3800-4800	-260~650	Strong	Better

TABLE 3: Composition of basalt powder.

Element content	(K[AlSi ₃ O ₈])	(MgCO ₃)	(XY(Si, Al) ₂ O ₆)	(Mg, Fe) ₂ [SiO ₄]
Powder (<0.075 mm)	67.40%	1.70%	19.70%	11.20%

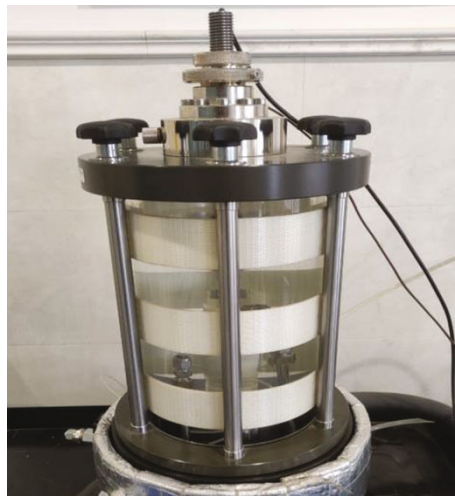


(a) Basalt fiber



(b) Basalt powder

FIGURE 2: Modified materials.



(a) Pressure chamber



(b) Control system

FIGURE 3: Triaxial test system.

TABLE 4: Test program.

Fiber length L_f (mm)	Basalt powder diameter D_f (mm)	Material content C_f (%)	Moisture content w (%)	Freeze-thaw cycles (time)	Confining pressure σ_c (kPa)
9	0.075	0 0.2 0.4 0.6	10.20	0 2 5 10 20 30	100 200 300

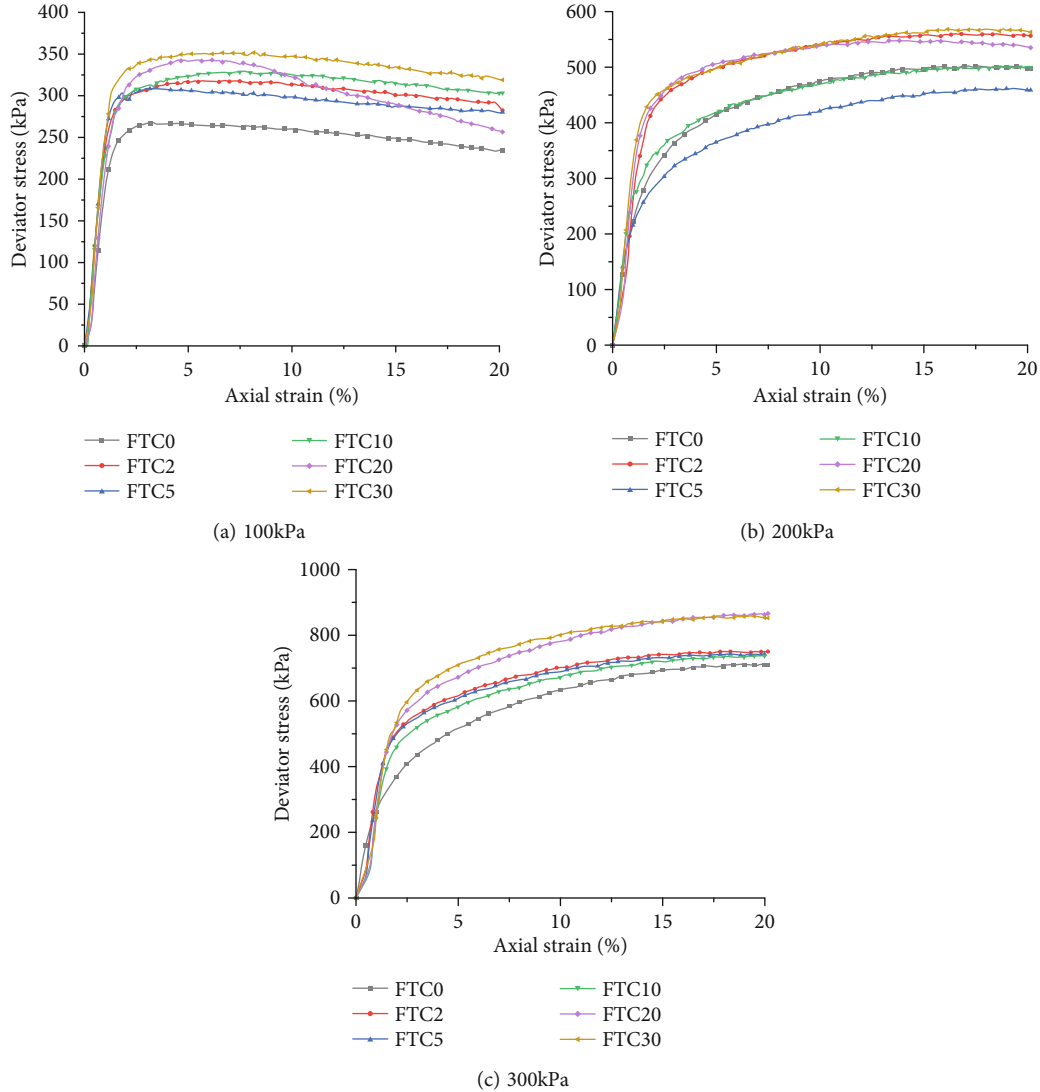


FIGURE 4: Stress-strain curve of normal soil.

Before preparing the sample, the soil was sieved through a 2 mm sieve and dried in an oven for at least 8 hours. It was then cooled to room temperature and mixed with 0.4% by mass basalt fiber and 0.4% by mass basalt powder. This mixture was sprayed with distilled water and kept in an airtight environment for 24 hours. Finally, the sample was prepared in five layers by the stratified sample preparation method, i.e., the soil samples were divided into five layers and compacted.

2.4. Test Program. The soil samples were subject to an unconsolidated and undrained conventional triaxial test

conducted using a servo motor-controlled dynamic triaxial test system (Figure 3) DYNNTTS (GDS Instruments, UK). The shear rate was set at 0.8 mm/min, and the test was stopped when the axial strain reached 20% of the soil sample. Three soil sample replicates were prepared for each experimental condition and put into the freeze-thaw cycle system. The time of each sample under freeze-thaw cycles was recorded; it was taken out when the number of freeze-thaw cycles reached a predetermined value. Samples were immediately tested at the confining pressure of 100 kPa, 200 kPa, and 300 kPa. The specific test program is as follows (Table 4).

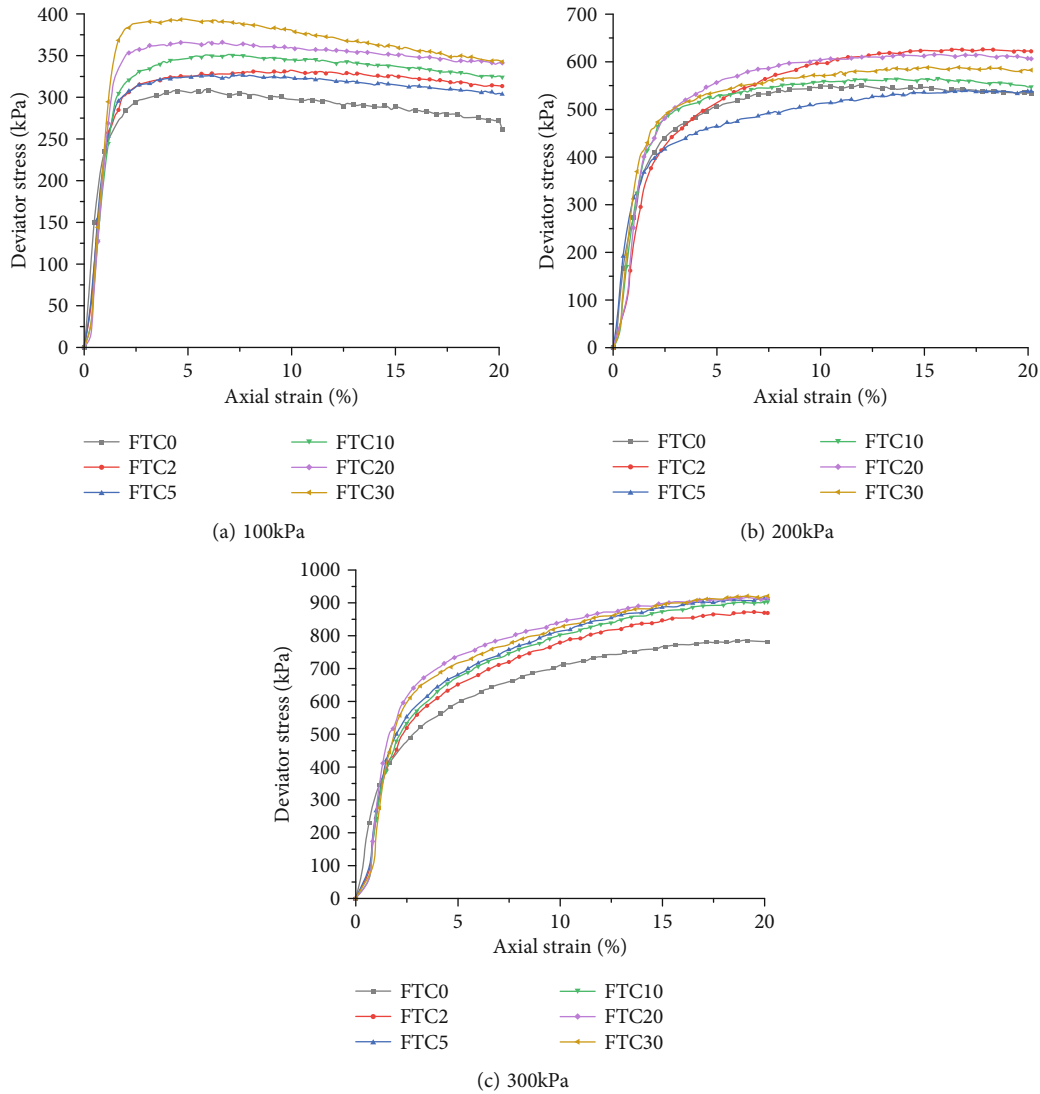


FIGURE 5: Stress-strain curve of basalt fiber soil.

3. Test Results and Discussion

3.1. Stress-Strain Curve

3.1.1. *Stress-Strain Curve of Normal Soil.* The stress-strain curve of the normal soil shows a weak strain softening type under low confining pressure (100 kPa), which gradually changes to a strain hardening type as the confining pressure increases (Figure 4). This results from circumferential compressive stress induced by confining pressure on the cylindrical soil specimen. Higher confining pressure increases the force exerted on the samples, reducing the development of weak sliding surfaces. As the number of freeze-thaw cycles increases, the strength of the soil changes as a result of being subject to different confining pressures. After 5 freeze-thaw cycles, the stress-strain curve of the soil is generally located in the lower position, which indicates that the response of the soil specimen to about 5 freeze-thaw cycles is more positive. At this time, the soil is in a sensitive state due to the continuous alternating phase change of water-ice, which

destabilizes the internal soil particles as a result of the continuous development and degradation of the cold-born structure. After 20 freeze-thaw cycles, the internal structure of the soil reaches a state of dynamic equilibrium, i.e., the distribution of the structure generated by freezing in the soil sample starts to stabilize and does not change significantly due to the increase in the number of freeze-thaw cycles, which is manifested in the macroscopic aspect as the strength of the soil gradually stabilizes.

3.1.2. *Stress-Strain Curve of Basalt Fiber Soil.* Basalt fiber soil (BF soil) behaves under confining pressure in a similar way to normal soil (Figure 5), indicating that the fundamental reason for determining the strength of the soil lies in the soil itself. The stress-strain curves of BF soil have obvious peaks in the range of 2.5%–5% at 100 kPa, and the peaks of curve are characterized by a forward shift with increasing numbers of freeze-thaw cycles. This is due to changes in the internal structure of the soil that accelerate the response of the soil to external loads resulting in an earlier peak. The spacing

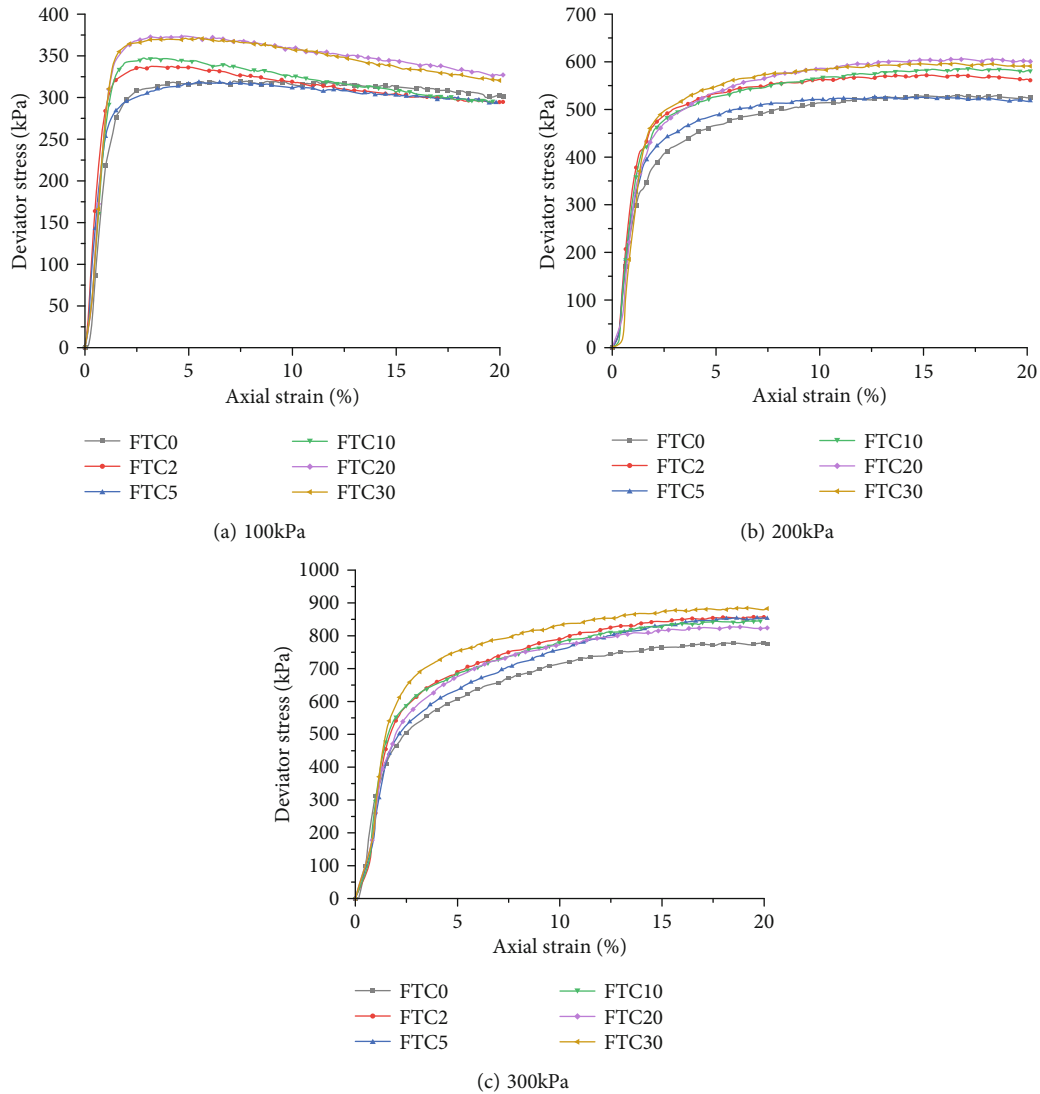


FIGURE 6: Stress-strain curve of basalt powder soil.

between stress-strain curves for different numbers of freeze-thaw cycles decreases with increasing confining pressure, as the interactions between the fibers' tensile action and the soil particles become more synergistic, thereby, weakening the effect of the freeze-thaw cycles on the internal structural of the soil. The stress-strain curves after 5 freeze-thaw cycles also appear in the lower position, which is consistent with the performance of the normal soil (Figure 5).

3.1.3. Stress-Strain Curve of Basalt Powder Soil. The stress-strain curves of the basalt powder soil (BP soil) are similar to those of both normal soil and BF soil (Figure 6). The stress-strain curves for 5 freeze-thaw cycles are similar when the confining pressure is 100 kPa and 200 kPa, while the stress-strain curve for 5 freeze-thaw cycles under 300 kPa confining pressure is slightly different, i.e., the soil strength increased compared with 0 times. However, the curve remains located primarily in the lower part of the curve, indicating that the state of the BP soil after about 5 freeze-thaw cycles is similar to that of the normal soil, (i.e., the

strength of BP soil was lower than that of 2 freeze-thaw cycles). The stress-strain curve distribution of BP soil under 200 kPa confining pressure is similar to that of BF soil under 300 kPa confining pressure. The final strength tends to a similar value for different numbers of freeze-thaw cycles, which is different from the state of BF soil under 200 kPa confining pressure. It is because the filling effect of basalt powder comes into play earlier than basalt fiber to stabilize the soil, leading to an earlier convergence of the curves.

3.2. Shear Strength. The shear strength of BF and BP soil is higher than that of the normal soil under all pressure conditions, suggesting the effectiveness of the modified materials (Figure 7). Basalt fiber and basalt powder improve the shear strength of the soil. Under the 100 kPa and 200 kPa confining pressure, the strength of the three soil types initially improved after 2 freeze-thaw cycles but then decreased after 5 freeze-thaw cycles. After 10 cycles, the shear strength of all soil types began increasing with additional cycles and gradually stabilized after 20 cycles. This phenomenon occurs

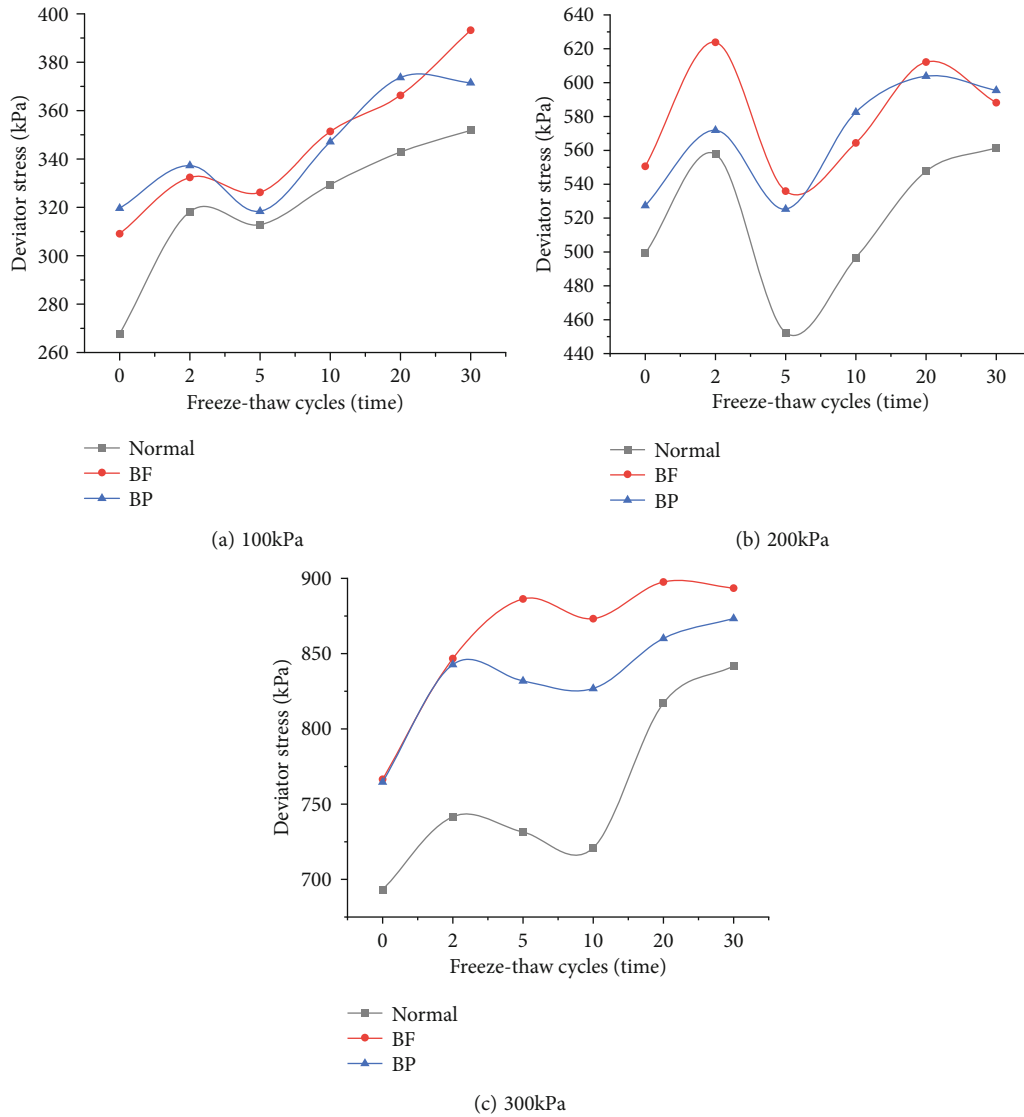


FIGURE 7: Shear strength.

because the internal structure of the soils gradually stabilized finally. After 30 freeze-thaw cycles, the shear strength of basalt fiber soil and basalt powder soil increased by 7.55% and 5.12%, respectively, compared with normal soil.

The initial enhancement in shear strength is likely due to the water-ice phase change compacting internal soil particles, that is, the development of the ice squeezes the soil particles and makes the soil denser. Between 2 and 10 freeze-thaw cycles, the internal structure of the soil starts to change structurally due to the phase change; as the number of freeze-thaw cycles reaches 5, the soil becomes more sensitive to external load and the structural changes within the soil are most drastic. This occurs because the first few cycles produced more pores in the soil, reducing overall soil stability. At 10–20 cycles, the shear strength of the soil begins to rise again, as the number of freeze-thaw cycles produces the weathering-like effect on the soil, filling the loose pore structure with the fractured material. Simultaneously, the cold-born structure squeezed the fractured soil. The strength does

not increase because the freeze-thaw cycle produces only a limited weathering effect that does not break or change the structure of the small particles inside the soil. The shear strength of the soil at 300 kPa is similar to that described above, with the only difference being that the shear strength of the soil reaches its lowest point at about 10 freeze-thaw cycles (instead of 5) due to the high confining pressure retarding the stress response of the soil, that is, at about 10 cycles, the weathering effect inside the soil decreases due to the increase of the confining pressure.

3.3. *Specimen Failure Characteristics.* The main damage to the samples after testing is compression of two ends and bulging in the middle (drum like), within wave-breaking or petal-like indentations appearing in the bulging area (Figure 8(b)). Sometimes, after low confining pressure, the damage appears cut like. The damage form of BF and BP soils is predominantly drum like suggesting that soil stability is improved after adding these two reinforcing materials.

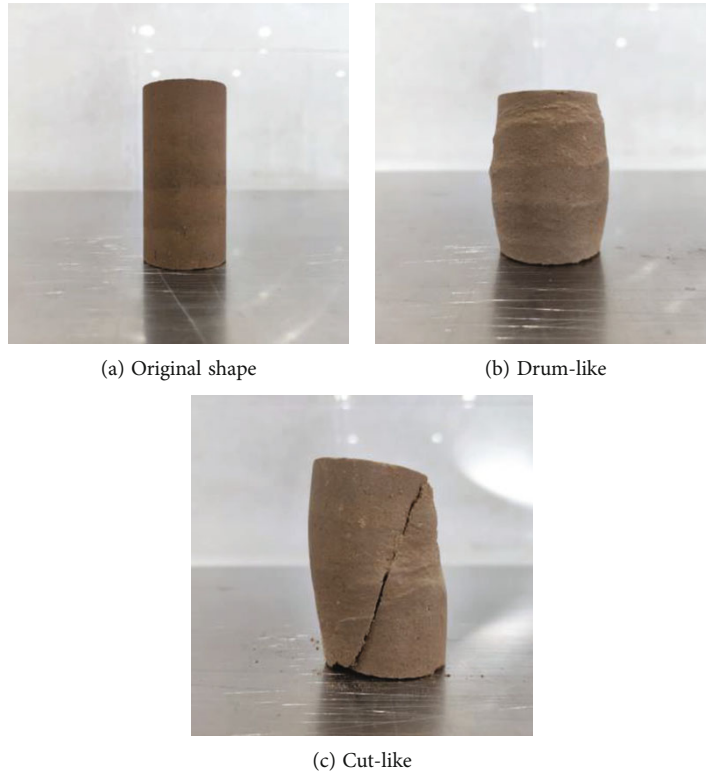


FIGURE 8: Destruction form.

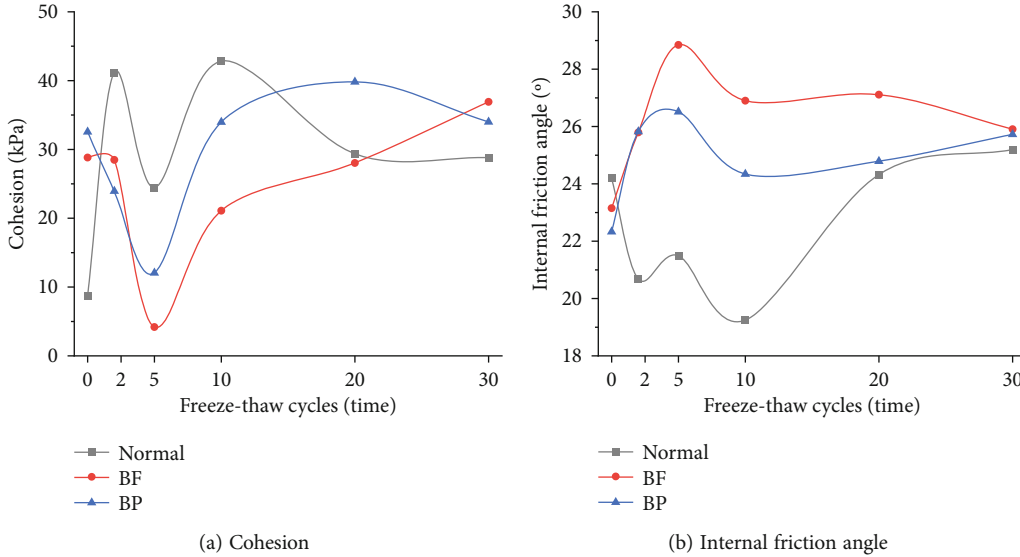


FIGURE 9: Cohesion and internal friction angle.

3.4. *Shear Strength Index.* The cohesion and internal friction angle of the soil samples are influenced by the number of freeze-thaw cycles (Figure 9). The cohesion of BF and BP soils was substantially increased compared to normal soil under 0 freeze-thaw cycles, although the cohesion decreases after 2 freeze-thaw cycles. On the other hand, the cohesion of normal soil increased after 2 cycles because the presence of admixtures weakens the extrusion effect of cold-born structures in the soil. After 5 freeze-thaw cycles, the cohesion

of all three soils was less than that at 2 cycles, a result of the pore space inside the soil becoming larger. After 20 freeze-thaw cycles, the cohesion of all three soils gradually stabilized. By 30 freeze-thaw cycles, the cohesive forces of the normal, BF, and BP soils increased by 229.91%, 28.12%, and 4.45%, respectively, compared with the soils that did not experience the freeze-thaw cycles.

The internal friction angle of admixture soil is smaller than that of normal soil when not experiencing freeze-thaw

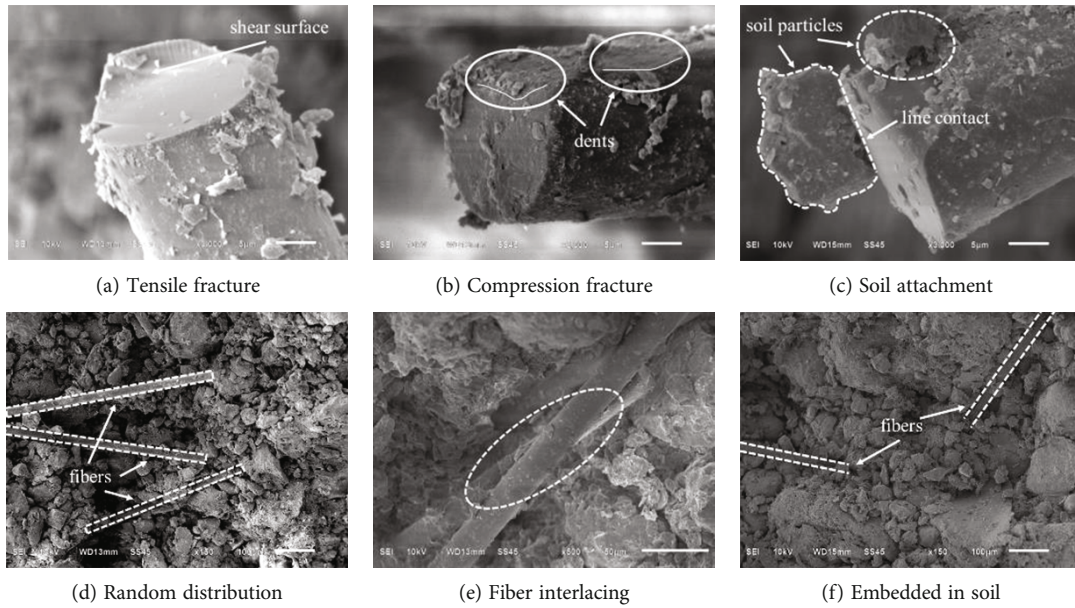


FIGURE 10: Detail of fiber.

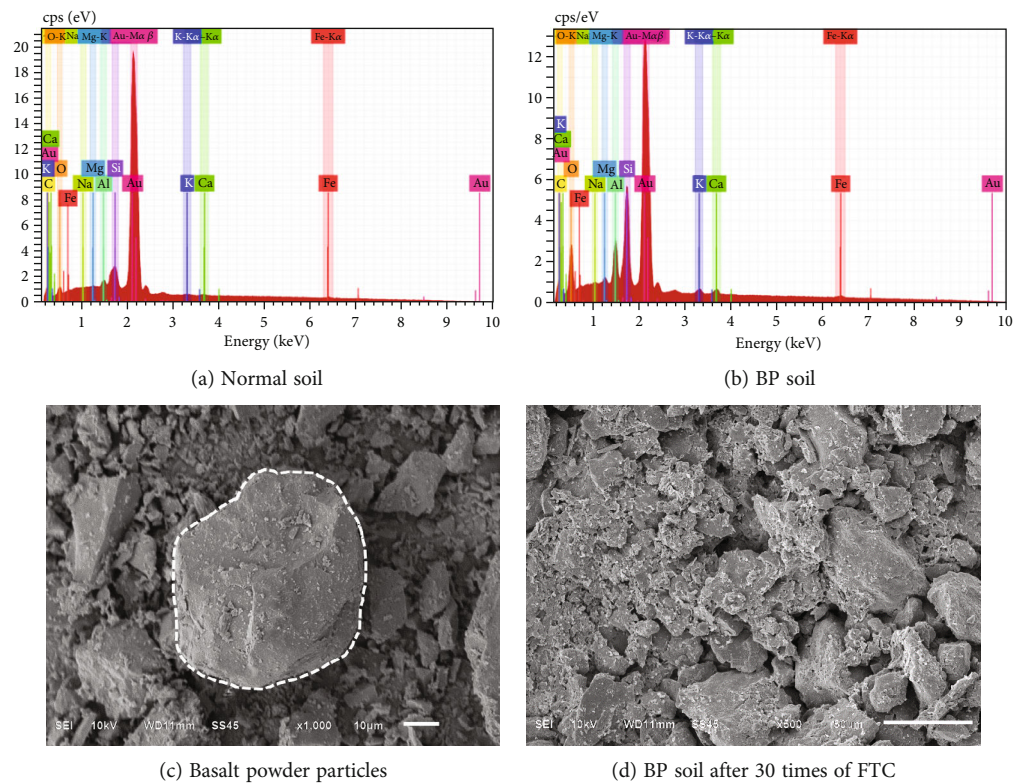


FIGURE 11: SEM and EDS test.

action (Figure 9). After being subjected to freeze-thaw cycles, the internal friction angle of the BF and BP soils both increase up to 5 freeze-thaw cycles, after which the internal friction angle starts to decrease and eventually becomes dynamically stable. The internal friction angle of the normal soil also gradually decreased and then stabilized after 20 freeze-thaw cycles. Overall, however, the internal friction angle of the normal soil did not change substantially after

repeated freezing and thawing, while the internal friction angles of BF and BP soil increased by 11.91% and 15.21% after 30 cycles, respectively.

4. Microstructural Analysis

Scanning electron microscope (SEM) test results revealed that the fiber damage was primarily in the form of tensile fracture

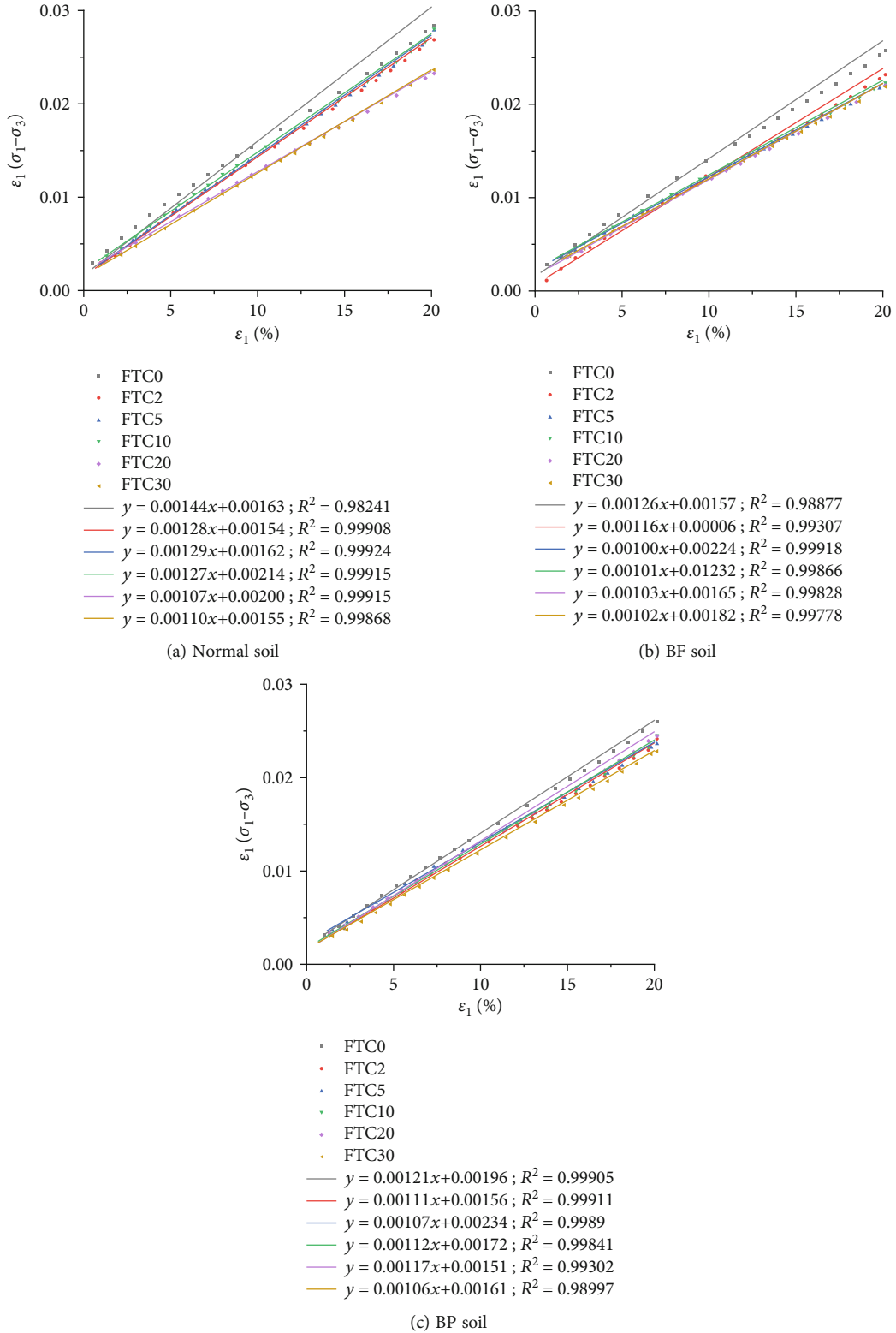


FIGURE 12: Hyperbolic fitting.

and compressive fracture (Figure 10). (Figure 10(a)) shows that the oblique section of the tensile fiber fracture is smooth and has a shear surface and this phenomenon occurs because the fibers mixed in the soil were subjected to tensile forces generated by external loads. (Figure 10(b)) shows the fiber

split by compression damage, where the cross-section is vertical and rough, and traces of pressure can be seen at the end of the fiber, which was because the soil particles squeeze the fibers and cause them to undergo lateral shear. (Figure 10(c)) shows the soil particles attached to the fiber

end, with the soil particles and fibers showing the characteristics of linear contact and surface contact. (Figures 10(d) and 10(f)) show the randomly distribution of fibers embedded in the soil, where the fibers are interlaced with each other, enhancing the macroscopic strength of the soil.

In order to study the effect of basalt powder on the microscopic level of the soil, SEM and energy dispersive spectroscopy (EDS) tests of BP soil had been done in this paper. SEM results show that the surface of basalt powder particles is relatively rough and basalt powder is difficult to distinguish after mixing into the soil (Figure 11). EDS tests show that the elemental contents of K, Al, Si, O, Ma, and Fe of the soil were enhanced after mixing with basalt powder, which is basically consistent with the composition table of basalt powder described in the previous paper (Table 3).

5. Stress-Strain Mathematical Model

The hyperbolic model was used to fit the stress-strain curves of the three soils under 300 kPa confining pressure [25], written as

$$\sigma_1 - \sigma_3 = \frac{\varepsilon_1}{a + b\varepsilon_1}, \quad (1)$$

where a and b are the test constants, whose values can be obtained from the test results plotted by straight line.

After mathematical transformation, the above formula can also be represented as

$$\frac{\varepsilon_1}{\sigma_1 - \sigma_3} = a + b\varepsilon_1. \quad (2)$$

Taking ε_1 as the abscissa and $\varepsilon_1/(\sigma_1 - \sigma_3)$ as the ordinate, the following results are obtained (Figure 12).

According to the fitted data, the overall slope of the fitted line is as follows: normal soil is greater than BF soil and BF soil is greater than BP soil. Overall, the model fits well.

6. Conclusion

- (1) After 30 freeze-thaw cycles, the mechanical strength of silty clay generally tended to increase and the shear strength of basalt fiber soil and basalt powder soil increased by 7.55% and 5.12%, respectively, compared with normal soil. The reinforcing effect of basalt fiber on this increase was generally better than that of basalt powder at the same dosing level of 0.4% by mass
- (2) Different numbers of freeze-thaw cycles have different effects on soil. After 2 freeze-thaw cycles, the soil strength improves, while strength subsequently decreases after 5–10 cycles, but reaches a dynamic equilibrium state higher than the initial level after 20 freeze-thaw cycles
- (3) With the increase of the number of freeze-thaw cycles, the cohesion and internal friction angles of normal vs. admixture soils differed. Cohesion ini-

tially decreased after 5 freeze-thaw cycles but tended to gradually increase and stabilize at higher than initial values as the number of freeze-thaw cycles increased further. Up to 5 freeze-thaw cycles initially increased the internal friction angle of the admixture soils, but the internal friction angle of the normal soil decreased over up to 10 cycles. However, subsequent freeze-thaw cycles tended to stabilize the internal friction angle of all three soil types at the same value

- (4) The strength of BF soil is improved after being subject to 30 of freeze-thaw cycles due to the interaction between the frictional force generated by the interlocking of fibers and the frictional force generated by the soil attached to the fibers. The strength of BP soil is improved after repeated freezing and thawing because of the combined effect of mechanical bite force and frictional force caused by the rough and uneven surface of basalt powder and the filling of some debris into the soil pores
- (5) The stress-strain curves of the three soil types can be simulated using the hyperbolic model. When data are fitted to this model, normal soil exhibited the largest slope, followed by BF and then BP soil

Data Availability

The data used to support the findings of this study are included within the article.

Conflicts of Interest

The authors declare that they have no conflicts of interest.

Acknowledgments

This work was supported by the National Natural Science Foundation of China (nos. 42161026 & 41801046), the Natural Science Foundation of Qinghai Province (no. 2021-ZJ-716), and the Transportation Science and Technology Project of Qinghai Province (no. 2018-02).

References

- [1] K. Fabian and A. Fourie, "Performance of geotextile-reinforced clay samples in undrained triaxial tests," *Geotextiles and Geomembranes*, vol. 4, no. 1, pp. 53–63, 1986.
- [2] D. R. Freitag, "Soil randomly reinforced with fibers," *Journal of Geotechnical Engineering*, vol. 112, no. 8, pp. 823–826, 1986.
- [3] T. Yetimoglu and O. Salbas, "A study on shear strength of sands reinforced with randomly distributed discrete fibers," *Geotextiles and Geomembranes*, vol. 21, no. 2, pp. 103–110, 2003.
- [4] C. Tang, B. Shi, W. Gao, F. Chen, and Y. Cai, "Strength and mechanical behavior of short polypropylene fiber reinforced and cement stabilized clayey soil," *Geotextiles and Geomembranes*, vol. 25, no. 3, pp. 194–202, 2007.

- [5] P. Kumar and S. P. Singh, "Fiber-reinforced fly ash subbases in rural roads," *Journal of Transportation Engineering*, vol. 134, no. 4, pp. 171–180, 2008.
- [6] M. Ghazavi and M. Roustaei, "The influence of freeze-thaw cycles on the unconfined compressive strength of fiber-reinforced clay," *Cold Regions Science and Technology*, vol. 61, no. 2–3, pp. 125–131, 2010.
- [7] M. Roustaei, A. Eslami, and M. Ghazavi, "Effects of freeze-thaw cycles on a fiber reinforced fine grained soil in relation to geotechnical parameters," *Cold Regions Science and Technology*, vol. 120, pp. 127–137, 2015.
- [8] A. Kumar, B. S. Walia, and J. Mohan, "Compressive strength of fiber reinforced highly compressible clay," *Construction and Building Materials*, vol. 20, no. 10, pp. 1063–1068, 2006.
- [9] S. M. Hejazi, M. Sheikhzadeh, S. M. Abtahi, and A. Zadhoush, "A simple review of soil reinforcement by using natural and synthetic fibers," *Construction and Building Materials*, vol. 30, pp. 100–116, 2012.
- [10] M. Ghazavi and M. Roustaei, "Freeze-thaw performance of clayey soil reinforced with geotextile layer," *Cold Regions Science and Technology*, vol. 89, pp. 22–29, 2013.
- [11] M. Olgun, "The effects and optimization of additives for expansive clays under freeze- thaw conditions," *Cold Regions Science and Technology*, vol. 93, pp. 36–46, 2013.
- [12] W. R. Azzam, "Behavior of modified clay microstructure using polymer nanocomposites technique," *Alexandria Engineering Journal*, vol. 53, no. 1, pp. 143–150, 2014.
- [13] W. R. Azzam, "Utilization of polymer stabilization for improvement of clay microstructures," *Applied Clay Science*, vol. 93–94, pp. 94–101, 2014.
- [14] R. Delinière, J. E. Aubert, F. Rojat, and M. Gasc-Barbier, "Physical, mineralogical and mechanical characterization of ready-mixed clay plaster," *Building and Environment*, vol. 80, pp. 11–17, 2014.
- [15] M. E. Orakoglu, J. Liu, and F. Niu, "Experimental and modeling investigation of the thermal conductivity of fiber-reinforced soil subjected to freeze-thaw cycles," *Applied Thermal Engineering*, vol. 108, pp. 824–832, 2016.
- [16] I. Kafodya and F. Okonta, "Effects of natural fiber inclusions and pre-compression on the strength properties of lime-fly ash stabilised soil," *Construction and Building Materials*, vol. 170, pp. 737–746, 2018.
- [17] M. Abbaspour, E. Aflaki, and N. F. Moghadas, "Reuse of waste tire textile fibers as soil reinforcement," *Journal of Cleaner Production*, vol. 207, pp. 1059–1071, 2019.
- [18] M. Bekhiti, H. Trouzine, and M. Rabehi, "Influence of waste tire rubber fibers on swelling behavior, unconfined compressive strength and ductility of cement stabilized bentonite clay soil," *Construction and Building Materials*, vol. 208, pp. 304–313, 2019.
- [19] A. J. Choobbasti, M. A. Samakoosh, and S. S. Kutanaei, "Mechanical properties soil stabilized with nano calcium carbonate and reinforced with carpet waste fibers," *Construction and Building Materials*, vol. 211, pp. 1094–1104, 2019.
- [20] A. Saygili and M. Dayan, "Freeze-thaw behavior of lime stabilized clay reinforced with silica fume and synthetic fibers," *Cold Regions Science and Technology*, vol. 161, pp. 107–114, 2019.
- [21] R. Tanzadeh, M. Vafaeian, and F. M. Yusefzadeh, "Effects of micro-nano-lime (CaCO_3) particles on the strength and resilience of road clay beds," *Construction and Building Materials*, vol. 217, pp. 193–201, 2019.
- [22] N. Tiwari, N. Satyam, and S. S. Kumar, "An experimental study on micro-structural and geotechnical characteristics of expansive clay mixed with EPS granules," *Soils and Foundations*, vol. 60, no. 3, pp. 705–713, 2020.
- [23] N. Tiwari, N. Satyam, and K. Singh, "Effect of curing on micro-physical performance of polypropylene fiber reinforced and silica fume stabilized expansive soil under freezing thawing cycles," *Scientific Reports*, vol. 10, no. 1, p. 7624, 2020.
- [24] A. Almajed, D. Srirama, and A. A. B. Moghal, "Response surface method analysis of chemically stabilized fiber-reinforced soil," *Materials*, vol. 14, no. 6, p. 1535, 2021.
- [25] J. M. Duncan and C.-Y. Chang, "Nonlinear analysis of stress and strain in soils," *Journal of the Soil Mechanics and Foundations Division*, vol. 96, no. 5, pp. 1629–1653, 1970.